# VISUAL ENHANCEMENT OF MICROCALCIFICATIONS AND MASSES IN DIGITAL MAMMOGRAMS USING MODIFIED MULTIFRACTAL ANALYSIS

by

***Tomislav M. STOJIĆ****

Faculty of Mechanical Engineering, University of Belgrade, Belgrade, Serbia

Scientific paper
DOI: 10.2298/NTRP1501061S

**Microcalcifications and masses, as breast tissue anomalies (deviations from observed background regularity), may be viewed as statistically rare occurrences in a mammogram image. After recognizing their principal common features – bright image parts not belonging to the surrounding tissue, with significant local contrast just around the edges – several modifications to multifractal image analysis have been introduced. Starting from a mammogram image, the proposed method creates corresponding multifractal images. Additional post-processing, based on mathematical morphology, refines the procedure by selecting and outlining only regions with possible microcalcifications and masses. The proposed method was tested through referent mammograms from the MiniMIAS database. In all cases involving the said database, the method has successfully enhanced declared anomalies: microcalcifications and masses. The results obtained have shown that the described procedure may provide visual assistance to radiologists in clinical mammogram examinations or be used as a preprocessing step for further mammogram processing, such as segmentation, classification, and automatic detection of suspected bright breast tissue lesions.**

*Key words: mammography, multifractal analysis, microcalcifications, masse, image processing*

## INTRODUCTION

Breast cancer is the most frequent malignant disease in women in Europe causing one in six of all deaths from cancers in the female population [1]. In the United States, according to the American Cancer Society reports [2], only lung cancer accounts for more cancer deaths in women.

Mammography is currently the most effective tool for the detection of breast cancer before clinical symptoms appear, since it offers high sensitivity and high specificity at low cost [2-5]. The older technique, screen-film mammography, records the breast image on a conventional X-ray film. After the acquisition, radiologists examine the X-ray films. The newest technology, full-field digital mammography, comprises direct conversion of the radiology image to the digital image without using the film. A clinical study involving 387 women and 1548 mammograms, has shown that digital mammography is superior both in terms of image quality and radiation dose over screen-film mammography [6].

Amongst others, two important radiological features in a mammogram are microcalcifications and masses as common early signs of possible breast cancer [2, 3]. Due to a higher attenuation of X-rays in relation to their surrounding, microcalcifications and masses are perceived as bright mammogram parts. Microcalcifications are small mineral deposits in the breast tissue [7]. Due to their small size (from 50 μm to 1.0 mm, typically 0.3 mm) [3, 7] the detection of microcalcifications is a difficult task [8, 9]. Masses or nodules are breast tissue anomalies composed of dense breast tissue [9]. In order to properly characterize a mass, radiologists generally rely on its contour [9]. The main reasons that hinder the detection of masses are changing shapes, size and density; poor contrast between masses and surrounding tissue; background tissue which is not uniform and often has similar characteristics to the masses [7, 9].

Mammograms are often considered as medical images with poor contrast. Conventional contrast enhancement algorithms and thresholding [10] are not quite appropriate methods since they globally change the entire image, not solely the particular details of interest. The main premise in this study is that human tissue, as many natural structures, is characterized by a

* Corresponding author; e-mail: tstojic@mas.bg.ac.rs

high degree of self-similarity, also referred to as fractality [11, 12]. In this context, self-similarity refers to images that have several parts looking as the whole image. The tissue anomalies are then considered as structural "defects", *i. e.*, as deviations from the global regularity of the background [12, 13].

A method for the segmentation of microcalcifications only, using properly adapted conventional multifractal image analysis, is proposed in [13]. Compared to other fractal methods that consider the irregularities of the measure only on a global scale, the procedures always ending with a single value or spectrum per analyzed image, this method considers each point of the image separately.

In this manner, one can establish a one-by-one correspondence between each image pixel and appropriate multifractal parameters. This also means that, after applying the method [13], one can find and segment only those image pixels with particular values of the multifractal exponent (usually denoted as $\alpha$) and its global distribution, commonly denoted as $f(\alpha)$. Therefore, the multifractal analysis may be performed in an inverse way: find parts in the image having particular values of $\alpha$ or $f(\alpha)$. This kind of processing may be defined as inverse multifractal analysis. The method also has the advantage of not being too computationally complex or too demanding in sampling statistics. The efficiency and usefulness of this approach in image segmentation was recognized by Levy Vehel [12, 14, 15], from INRIA, France, and a corresponding program was embedded in the well-known Fraclab software [14].

The author has also proposed a method for the segmentation of clusters with microcalcifications based on modern mathematical morphology [8, 16]. Both approaches, multifractal and morphology, are presented in brief in [16] and certain comparisons between the methods considered.

In this paper, the basic multifractal algorithm for the segmentation of microcalcifications only [13] is extended to include the visual enhancement of masses too. The basic premise is that masses, as well as microcalcifications, may be considered as defects or rare anomalies of the breast tissue. An additional similarity is that both types of anomalies are observed as parts of mammograms brighter than their surroundings due to the higher attenuation of X-rays. Additionally, by introducing noise filtering at the preprocessing level and proper morphological operations at the post-processing level, the visual enhancement of masses is improved. The newly proposed method could be used for the visual enhancement and segmentation of both masses and microcalcifications. The efficiency of the proposed method has been tested through referent mammograms from the mammographic image analysis society (MiniMIAS) referent database [17] and some results presented in this work.

## METHOD DESCRIPTION

### Multifractal image analysis basics

Artificially generated fractal structures (monofractals) are described by the same fractal dimension in whole scales [11, 18]. Natural objects also exhibit self-similarity, but only in a statistical sense. The fractal dimension of these structures (multifractals) varies with the observed scale [18-22].

The quantitative description of a multifractal property can be derived in several ways. Due to its simplicity, the box-counting method is very often used. Let the structure $S$ be divided into non-overlapping boxes $S_i$ of size $\varepsilon$ such that $S = {}_iS_i$. Each $S_i$ box is characterized by a specific measure, $\mu(S_i)$, and the boxes may be assumed as measure domains. The quantity

$$\alpha_i \quad \frac{\ln[\mu(S_i)]}{\ln \varepsilon} \tag{1}$$

is known as the coarse Hoelder exponent of the subset $S_i$. If $\varepsilon$ tends to zero, the coarse Hoelder exponent approaches the limiting value $\alpha$ at the observed point

$$\alpha \quad \lim_{\varepsilon \to 0} \alpha_i \tag{2}$$

Parameter $\alpha$ describes the local regularity of the structure. In the structure as a whole there are many points with the same value of parameter $\alpha$. The next step is to find the distribution of $\alpha$, *i. e.* determine the function $f(\alpha)$, known as the multifractal (MF) spectrum. Function $f(\alpha)$ describes the global regularity of the observed structure [11, 18]. The multifractal spectrum can be viewed as the fractal dimension over the subsets characterized by $\alpha$

$$f_\varepsilon(\alpha_i) \quad \frac{\ln[N_\varepsilon(\alpha_i)]}{\ln \varepsilon} \tag{3}$$

where, $N_\varepsilon(\alpha_i)$ is the number of boxes $S_i$ containing the particular value of $\alpha_i$. From expression (3) one can obtain the limiting value

$$f(\alpha) \quad \lim_{\varepsilon \to 0}[\, f_\varepsilon(\alpha)] \tag{4}$$

The MF spectrum $f(\alpha)$ calculated as above is also known as the Hausdorff dimension of the $\alpha$ distribution.

Upon finding the values of $\alpha$ one may create an "$\alpha$-image" – a matrix of the same dimensions as an initial image, but comprised of values of $\alpha(m, n)$ with one-by-one correspondence to the image pixels. This means that, at position $(m, n)$, an "$\alpha$-image" has the value of $\alpha(m, n)$ instead of the original pixel gray level. From this matrix (or image), the MF spectrum $f(\alpha)$, also in matrix form, $f(m, n) = f[\ (m, n)]$, can be estimated. First, continuos exponents are discretized into $R$ values of $\alpha_r$

$$\alpha_r \quad \alpha_{\min} \quad (r \quad 1)\Delta\alpha_r\,, \quad r \quad 1, 2, \ldots, R \tag{5a}$$

In [13] the uniform division is used with

$$\Delta\alpha_r \quad \Delta\alpha \quad \frac{(\alpha_{\max} \quad \alpha_{\min})}{R} \tag{5b}$$

If the actual value of $\alpha$ is within the subrange $r$, *i. e.*, if $\alpha_r \quad \alpha < (\alpha_r + \Delta\alpha)$, it is replaced by $\alpha_r$. Such an $\alpha$-image is covered by a regular grid of boxes with integer box sizes $j = 1, 2, \ldots$ The boxes containing at least one value of $\alpha_r$ are counted, giving the number $N_j(\alpha_r)$. Boxes of different sizes are recursively taken into account and corresponding Hausdorff measures calculated for each image pixel according to expression (3) as

$$f_j(\alpha_r) \quad \frac{\ln N_j(\alpha_r)}{\ln j}, \; j \quad 1, 2, \ldots \tag{6}$$

Finally, from a set of discrete points in the bi-logarithmic diagram of $\ln N_j(\alpha_r)$ *vs.* $-\ln j$, the MF spectrum $f(\alpha)$ is estimated from linear regression. The procedure is repeated for the entire $\alpha$-matrix, thus obtaining the "$f(\alpha)$-image" – a matrix filled by pixel-wise values of $f(\alpha)$. As in the "$\alpha$-image", in an "$f(\alpha)$-image" at position $(m, n)$, the $f[\alpha(m, n)]$ value is estimated instead of the pixel gray level [13].

Different measures $\mu_i(m, n)$, may be used for estimating $\alpha$. Some of the most frequently used measures are [12]

$$\text{Maximum:} \quad \mu_i(m,n) \quad \max_{(k,l) \; \Omega} g(k,l) \tag{7a}$$

$$\text{Minimum:} \quad \mu_i(m,n) \quad \min_{(k,l) \; \Omega} g(k,l) \tag{7b}$$

$$\text{Sum:} \quad \mu_i(m,n) \quad \sum_{(k,l) \; \Omega} g(k,l) \tag{7c}$$

where $i$ is the size of a measure domain around the observed pixel $(m, n)$, $\Omega$ is a set of all pixels $(k, l)$ within a measure domain, and $g(k, l)$ is a grayscale intensity at point $(k, l)$.

## Modification of multifractal analysis to visual enhancement of microcalcifications and masses

Microcalcifications and masses, due to a higher attenuation of X-rays than the immediate background tissue, correspond to image parts brighter than their surrounding [3, 23]. Microcalcifications are seen as small bright spots not belonging to the background tissue. In geometrical interpretation, they are singular sets of points. Sharp changes in the gray-level appear just around the edges of microcalcifications [24, 25]. Masses are bright and relatively smooth surfaces in a mammogram, significantly larger than microcalcifications. Masses are quite subtle, often occur in the dense areas of the breast tissue, with smoother boundaries than microcalcifications, and in different shapes: circumscribed, speculated (or stellate), lobulated or ill-defined [23, 26].

With the common features of microcalcifications and masses in mind, *i. e.*,: (1) that they are image parts brighter than their immediate surroundings, (2) not belonging to the background tissue (rare events in a statistical sense), with (3) significant local contrast just around their edges, exhibiting (4) different sizes and shapes, we can infer the guidelines for the adaptation of multifractal analysis targeted to the visual enhancement of microcalcifications and masses. From multifractal images, $\alpha$ and $f(\alpha)$, upon once established one-by-one pixel-wise correspondence with the original image, one should be able to select possible masses and microcalcifications as objects made of pixels having both high $\alpha$ (high local contrast) and low $f(a)$ (rare events) values.

The capacity measure "minimum", relation 7(b), applied to an inverted (negative) mammogram image, is well suited to emphasize local image regularity [13]. Namely, in a negative image, bright lesions (possible masses and microcalcifications) migrate to the dark region where the local contrast, described by the ratio $\Delta \ln \mu / \Delta\mu$, is very high. In this way, one can obtain the effect of the "logarithmic amplifier" which strongly enhances just the small gray-level variations in the dark zone of the inverted image (*i. e.*, bright zone of the original image). From the plot of $\ln \mu$, fig. 1, it is evident that local contrast expressed by $\Delta \ln \mu / \Delta\mu$ is very high in the dark-level domain (low $\mu$) and very low in the light-level domain (high $\mu$), which is directly opposite to the need of enhancing bright details. However, if one considers the inverted image, described as a complement of the original image, bright anomalies (possible masses and microcalcifications) will migrate to the dark region under the strong influence of the "logarithmic amplifier". This procedure does not reduce the sensitivity within regions in the middle gray, while in the bright zone of the inverted image (dark zone of an original image), the contrast between anomalies and surrounding tissue is naturally high enough.

When enhancing a particular object, better results are obtained if the shape of the measure domain is well adapted to the object. Taking into consideration the most common shape of masses and microcalcifications, one can find that the disk-shaped domain is well suited [7, 10, 13].

The multifractal spectrum is determined by the box-counting method according to (6). Since the goal is to favor singularities, *i. e.*, high frequency components in the $\alpha$ distribution, it is preferable to use small boxes sized $j = 1$ to $j = 16$ $\alpha$-pixels [13]. If the box size is large enough, the number of non-empty boxes tends to saturation: it may remain unchanged although the box sizes increase. Further on, points on the bi-logarithmic plot $\ln N_j(\alpha_r)$ *vs.* $-\ln j$ stay on the horizontal

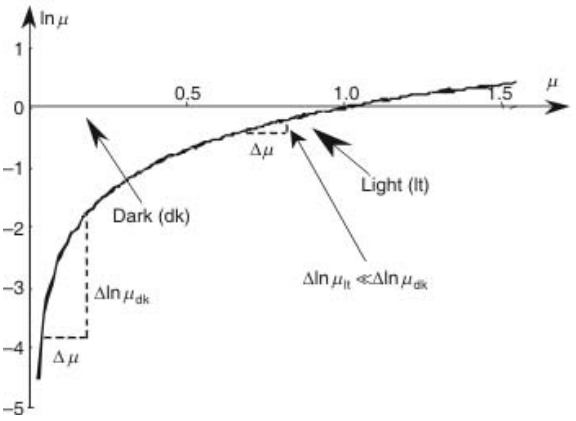


**Figure 1. Plot of ln illustrates the effect of the "logarithmic amplifier" in the dark-level domain**

line, significantly reducing the resolution of calculated $f(\alpha)$ values. To the contrary, by using smaller boxes, the number of non-empty boxes significantly varies with the changes in the dimensions of the box, preventing saturation and enabling a high resolution of estimated $f(\alpha)$ values [13].

The number of $\alpha$ subranges, denoted as $R$ in expression (5a), also influences the accuracy of the MF spectrum. A small number of $\alpha$ subranges yields a smooth spectrum, but with a small resolution. Conversely, too many subranges produce a saw-toothed ("erratic") spectrum, albeit more detailed. In this research, as a compromise solution, the value of $R = 100$ is adopted.

## Application of the modified multifractal algorithm

The efficiency of the suggested algorithm has been verified through referent mammograms from the MiniMIAS database [17]. All mammograms in the database have the same, 1 MB size, same 200 microns spatial resolution, same dimension (1024 1024 pixels) and same 8-bit gray-level pixel depth. Only mammograms with declared masses and microcalcifications have been selected from the whole set. For better visualization and computational purposes, only parts (sized 256 256 pixels) of the whole mammograms containing zones of declared anomalies were under exanimation. Multifractal quantities, $\alpha$ and $f(\alpha)$, were calculated by the previously described procedure. Original images were first inverted and then the capacity measure "minimum" used over disk-shaped measure domains sized 1, 3, and 5 image pixels. The number of subranges was $R = 100$, and the covering box sizes were $j = 1, 2, 4, 6, 8, 10, 12, 14$, and 16 $\alpha$-pixels.

The mammograms in the MiniMIAS database, as most other medical images, contain different types of noises [27]. Any potentially suitable noise removal technique must preserve small contrast changes just around the edges of the lesions, because the visual detection of masses and microcalcifications generally relies on the existence of this boundary contour. However, every filtering changes the "fractality" of the filtered image part. In [13] no filtering is used because microcalcifications are usually so small that applying even small-sized filters could completely remove or degrade (attenuate) the contrast just around their edges. Masses are significantly larger and intensive simulations showed that noise removal by a small-sized median filter is effective. The median filter is a simple and efficient tool in removing noise while preserving the edges [10]. Additionally, median filtering homogenizes the texture of the background tissue and the mass itself without a significant degradation of the grey-level contrast between them.

After the application of the modified multifractal algorithm, some morphological postprocessing is needed [28]. A successive morphological closing and opening via a small disk- shaped structuring element [8, 10] is suggested. By morphological closing (dilation followed by erosion), the holes within the segmented objects are filled and the unlinked contours connected. Then, by applying opening (erosion followed by dilation), objects smaller than the used structuring element are completely removed. Objects deleted in this way mostly correspond to the bright artefacts generated by some internal and/or external sources, such as film emulsion failures and X-ray detector noise [13, 27]. Finally, the contour lines around the segmented objects are obtained as lines at the boundaries of the objects comprised of border pixels only. By superimposing these borderlines to the original image, segmented details are strongly visually enhanced. As for masses, it is suitable to mark the largest suspicious region, possibly the suspicious mass at first and after that, if needed, to mark the subsequent ones. This can be easily accomplished by pinpointing the inner area of the object bounded by its contour line [10].

## RESULTS

### Mammogram with microcalcifications

In fig. 2(a) mammogram mdb256.pgm from the MiniMIAS database is shown. Its part (256 256 pixels) around the declared cluster of microcalcifications is depicted in fig. 2(b). The MF spectrum $f(\alpha)$ of the image in fig. 2(b) is plotted in fig. 2(c), and corresponding $\alpha$ and $f(a)$ images presented in figs. 2(d) and (e), respectively.

Microcalcifications are local tissue anomalies, parts of a mammogram not belonging to the background tissue. From the multifractal standpoint, they have both high $\alpha$ and low $f(\alpha)$ values, because, they represent sharp local changes and rare events. This is easily noticeable in figs. 2(d) and (e) – microcalcifications are represented as bright details (high values) in an $\alpha$-image and as dark ones (low values) in an $f(\alpha)$ image.

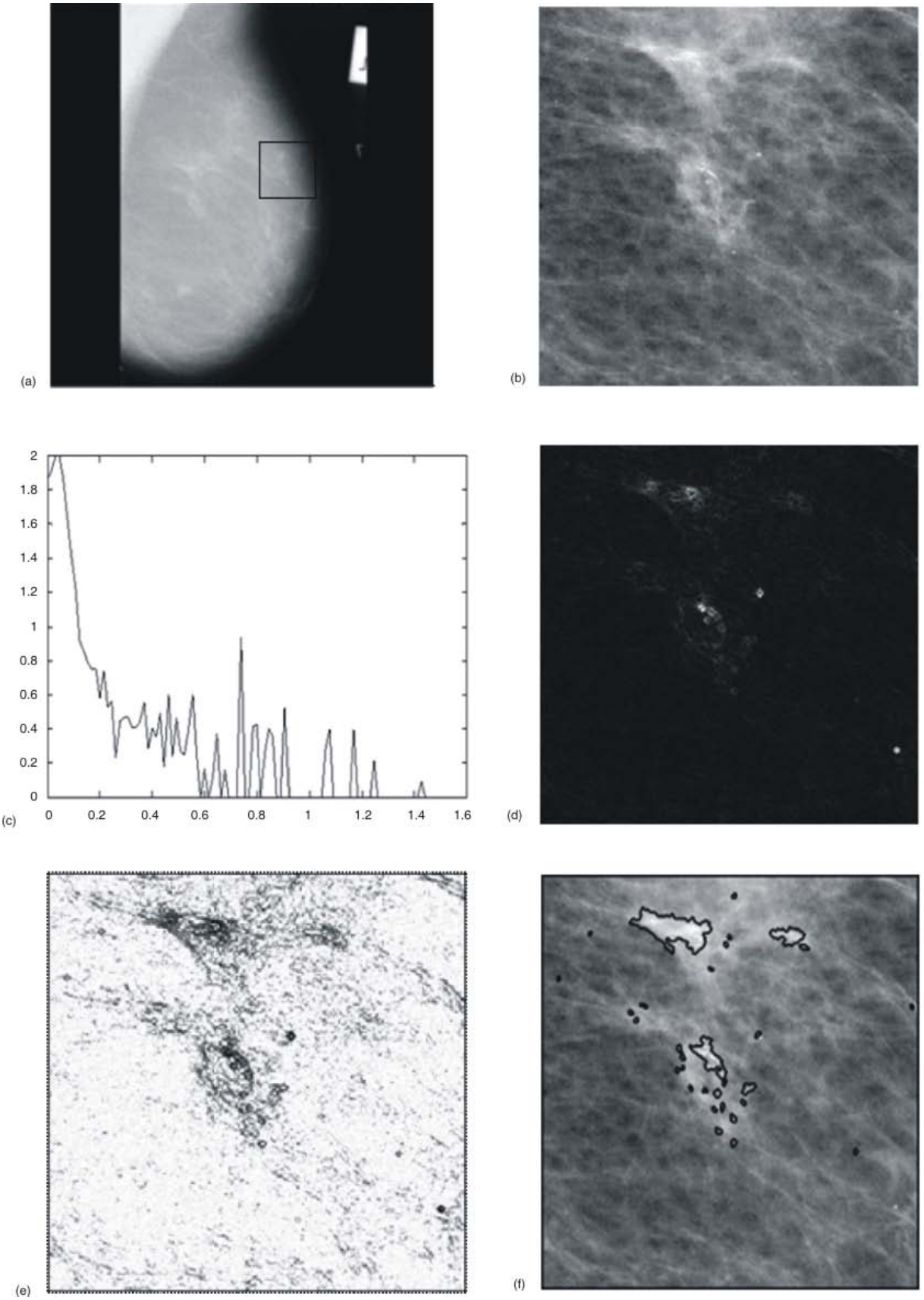


**Figure 2. (a) Original mammogram mdb256.pgm from the miniMIAS database; (b) part of mammogram mdb256.pgm corresponding to the black solid square in (a) with declared cluster of microcalcifications; (c) multifractal spectrum of the image in (b); (d) an $\alpha$ image obtained from (b); (e) corresponding $f(\alpha)$ image of a mammogram part in (b); (f) superimposed contour lines around segmented objects after morphological post-processing obtained from $f(\alpha)$ image by selecting pixels with $0 \quad f(\alpha) < 1$**

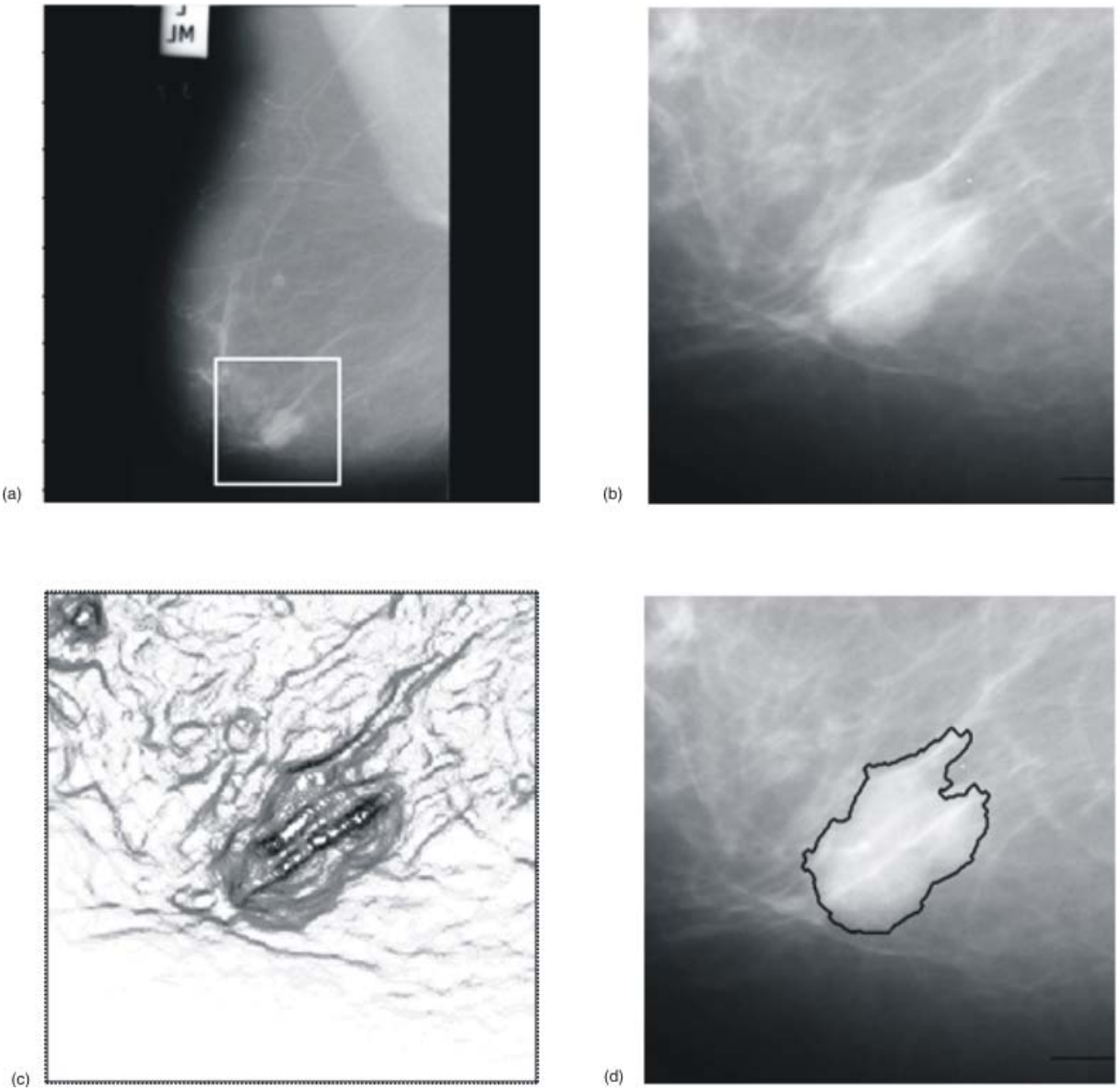


**Figure 3. (a) Original mammogram mdb005.pgm; (b) part of the mammogram within a white solid square from (a) with a mass; (c) $f(\alpha)$ image; (d) contour line superimposed onto the original image after morphology post-processing applied to a segmented $f(\alpha)$ image within the range 0 $f(\alpha) < 1$**

Note that in the $\alpha$-image the background is not purely black, but our visual system is not able to distinguish small gray-level variations in the dark domain. Geometrically, microcalcifications are seen as singular sets of points not belonging to the more complex structures (such as line, texture, surface), thus having topological dimension smaller than 1 [11, 20].

Once obtaining $\alpha$- and $f(\alpha)$ images, we can select the desired parts from an original image by extracting pixels having particular values of $\alpha$ and $f(\alpha)$. Referring to the multifractal spectrum in fig. 2(c), we can select image pixels from the desired range of $f(\alpha)$ values, in this case 0 $f(\alpha) < 1$, and after refining the segmentation by using successive morphological closings and openings, we can obtain contour lines around the segmented details. These contour lines have been superimposed onto the original image from fig. 2(b), as displayed in fig. 2(f), pointing to a cluster of microcalcifications. By changing the $f(a)$ range, we can interactively choose the appropriate segmentation level for each particular case.

**Mammograms with masses**

Mammogram mdb005.pgm from the MiniMIAS database with a clinically approved mass is shown in fig. 3(a). A part of this mammogram (256 256 pixels) corresponding to the white square in fig. 3(a) is depicted in fig. 3(b) and the $f(\alpha)$ image in fig. 3(c).

Before applying the proposed algorithm, the mammogram part from fig. 3(b) was preprocessed us-

ing a median filter with a window size of 5 5 pixels. Multifractal images, $\alpha$ and $f(\alpha)$, were calculated using the same procedure and parameters as in the previous case with microcalcifications.

As already noted, masses are regions of dense breast tissue, brighter than their surroundings, with sharp gray-level changes just around the edges. Statistically, masses are rare events in an mammogram image, thus having a low $f(\alpha)$ value. In fig. 3(d), a mammogram part with a superimposed contour line obtained from a $f(\alpha)$ image in fig. 3(c) by selecting pixels with 0 $f(\alpha) < 1$ is shown. Additionally, after morphological post-processing (closings followed by openings), only the contour line around the largest segmented object (a mass) is depicted.

The last case refers to mammogram mdb010.pgm with a mass approved by the MiniMIAS database, as shown in fig. 4(a). In fig. 4(b), a cropped mammogram part within a white square (256 256 pixels) with a superimposed contour around the largest segmented object is depicted. Before analysis, the cropped part was preprocessed using a median filter (5 5 pixels). The segmentation was carried out from a $f(\alpha)$ image by selecting pixels with 0 $f(\alpha) < 1$. After segmentation, a morphological closing followed by an opening was applied.

Although the calculation of the multifractal spectrum is time-consuming, particularly for large images, from a once obtained multifractal image radiologists gain the freedom to change the level of segmentation by setting the range of $f(\alpha)$ values, thus pinpointing the desired regions which may contain microcalcifications and masses.

This paper considers the application of the same multifractal algorithm for enhancing two essentially different breast tissue anomalies: microcalcifications and masses. It has shown that, with minor modifications, the multifractal algorithm for the segmentation of microcalcifications can be extended to enhance the masses of interest. The basic premise is that the masses, as well as microcalcifications, may be considered as defects, anomalies of the breast tissue and, hence, rare events in a statistical sense. An additional similarity is the fact that, due to the higher attenuation of X-rays, both types of anomalies are observed as mammogram parts brighter than their surroundings. In order to improve the segmentation of the contour line around the mass, some additional morphological post-processing is needed. After contour line segmentation, it is quite possible to determine certain properties of the selected object, such as spatial properties (size, different shape parameters, *etc*.), texture (kind and quality of textures) or fractal properties (local and global regularity of the object structure). Adding fractal parameters to existing feature vectors may improve algorithms for automatic classification in mammography, such as the classification of masses and clusters with benign or malignant microcalcifications.

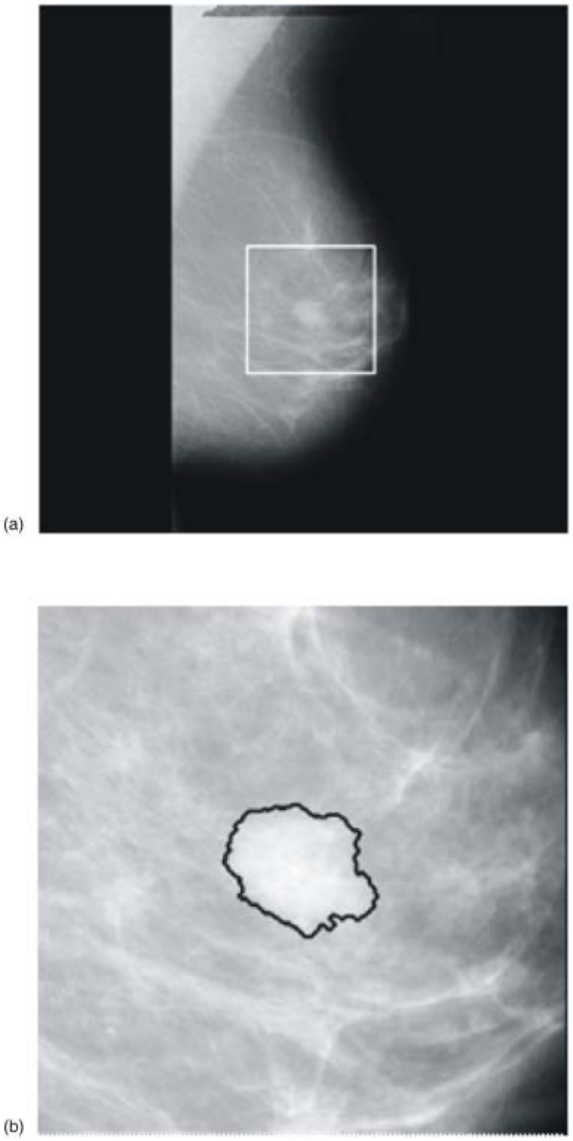


**Figure 4. (a) Original mammogram mdb010.pgm from the MiniMIAS database and (b) contour line around the segmented mass superimposed onto the mammogram part corresponding to the white square in (a)**

## CONCLUSIONS

In the domain of visual enhancement, microcalcifications are small bright spots not belonging to the background tissue, usually in the form of clusters, characterized by a sharp change of local contrast at their very edges. In multifractal terminology, these features are defined by the high values of the Hoelder exponent (high local changes) and low values of its distribution $f(\alpha)$ (rare events in a global sense).

Considering the masses as bright irregular image parts differing from the surrounding tissue, statistically representing rare events, the method for the visual enhancement of microcalcifications has been extended to include the enhancement of the said masses.

By introducing median noise filtering at the preprocessing level, as well as morphological closing and opening followed by object boundary extraction at the post-processing level, the segmentation of masses is significantly improved.

Note that the calculation of the multifractal spectrum is time-consuming, particularly for large images. But, from a once obtained multifractal image radiologists gain the freedom to change the level of segmentation by setting the range of $\alpha$ and/or $f(\alpha)$ values in order to find the desired regions containing bright anomalies, *i. e.* possible microcalcifications and masses. Objects enhanced in this way are not only microcalcifications and masses, but also, details brighter than the surroundings which can be considered as structural "defects", *i. e.* as deviations from the global regularity of the background. By introducing morphological post-processing, we may remove isolated details which, most likely, should not be classified as tissue anomalies.

The efficiency of the proposed method was tested via mammograms from the MiniMIAS database. In all instances, the method successfully enhanced the declared anomalies, masses and microcalcifications.

The method proposed here may be used as a visual assistance in mammogram analysis or embedded as part of a more complex expert system for mammogram examination or automatic detection of masses and microcalcifications aimed at obtaining information about local and global regularity/fractality of the segmented objects.

## REFERENCES

[1] ***, Health Statistics – Atlas on Mortality in the European Union, 2009, http://epp.eurostat.ec.europa.eu
[2] ***, Breast Cancer Facts and Figures, American Cancer Society, 2014, http://www.cancer.org/.
[3] Sakka, E., Prentya, A., Kotsourise, D., Classification Algorithms for Microcalcifications in Mammograms (Review), *Oncology Reports, 15* (2006), 4, pp. 1049-1055
[4] Praskalo, J., *et al*., A Survey of Short-Term and Long-Term Stability of Tube Parameters in a Mammography Unit, *Nucl Technol Radiat, 29* (2014), 4, pp. 321-325
[5] Stanković, K., Vujisić, M., Influence of Radiation Energy and Angle of Incidence on the Uncertainty in Measurements by GM Counters, *Nucl Technol Radiat, 23* (2008), 1, pp. 41-42
[6] Stantić, T., *et al.*, Screen-Film Versus Full-Field Digital Mammography: Radiation Dose and Image Quality in a Large Teaching Hospital, *Nucl Technol Radiat, 28* (2013), 4, pp. 398-405
[7] ***, Advanced Algorithmic Approaches to Medical Image Segmentation, (Eds. J. Suri, S. Setarehdan, S. Singh), Springer-Verlag, 2002, p. 636
[8] Reljin, B., *et al*., Computer Aided System for Segmentation and Visualization of Microcalcifications in Digital Mammograms, *Folia Histochemica Et Cytobiologica, 47* (2009), 3, pp. 525-532
[9] Soares, F., *et al*., Towards the Detection of Microcalcifications on Mammograms through Multifractal Detrended Fluctuation Analysis, *Proceedings*, IEEE PACRIM Conference, University of Victoria, Victoria, B. C., Canada, 2009, pp. 677-881
[10] Gonzales, R., Woods, R., Digital Image Processing (3rd ed.), Prentice Hall, New Jersey, 2008, p. 954
[11] Mandelbrot, B., The Fractal Geometry of Nature, W. H. Freeman, Oxford, 1983, p. 460
[12] Levy Vehel, J., Mignot, P., Multifractal Segmentation of Images, *Fractals, 2* (1994), 3, pp. 379-382
[13] Stojić, T., Reljin I., Reljin B., Adaptation of Multifractal Analysis to Segmentation of Microcalcifications in Digital Mammograms, *Physica A: Statistical Mechanics and its Applications, 367* (2006), pp. 494-508
[14] Fraclab, http://fraclab.saclay.inria.fr/people
[15] Levy Vehel, J., Introduction to the Multufractal Analysis of Images, Technical report INRIA, 1996
[16] Stojić, T., Reljin, B., Enhancement of Microcalcifications in Digitized Mammograms: Multifractal and Mathematical Morphology Approach, *FME Transactions*, *38* (2010), 1, pp. 1-10
[17] Suckling, J., The MiniMIAS Database, Mammographic Image Analysis Society – MIAS, www.wiau.man.ac.uk/services/MIAS/MIAScom.html
[18] Evertsz, C., Mandelbrot, B., Multifractal Measures, Appendix B in: H. Peitgen, H. Jurgens, P. Andrews Chaos and Fractals, Springer, 1992., p. 864
[19] Turner, M. J., Blackledge, J. M., Andrews, P. R., Fractal Geometry in Digital Imaging, Academic Press,1998, p. 328
[20] Reljin, I., Reljin, B., Fractal Geometry and Multifractals in Analyzing and Processing Medical Data and Images, *Archive of Oncology, 10* (2002), 4, pp. 283-293
[21] Iannaccone, P., Khokha, V., Fractal Geometry in Biological Systems, CRC Press, 1996, p. 384
[22] Pesquet-Popescu, B., Levy Vehel, J., Stochastic Fractal Models for Image Processing, *IEEE Signal Processing Magazine, 19* (2002), 5, pp. 48-62
[23] Cheng, H. D., *et al*., Approaches for Automated Detection and Classification of Masses in Mammograms, *Pattern Recognition, 39* (2006), 4, pp. 646-668
[24] Bakic, P. R., *et al*., Mammogram Synthesis Using a 3-D Simulation, *Medical Physics, 29* (2002), 9, pp. 2140-2151
[25] Carton, A.-K., *et al*., Development and Validation of a Simulation Procedure to Study the Visibility of Micro Calcifications in Digital Mammograms, *Medical Physics, 30* (2003), 8, pp. 2234-2240
[26] Kekre, H. B., Sarode, T. K., Gharge, S. M., Tumor Detection in Mammography Images using Vector Quantization Technique, *International Journal of Intelligent Information Technology Application, 2* (2009), 5, pp. 237-242
[27] Maitra, I. K., Nag, S., Bandyopadhyay, S. K., Automated Digital Mammogram Segmentation for Detection of Abnormal Masses Using Binary Homogeneity Enhancement Algorithm, *Indian Journal of Computer Science and Engineering*, 2 (2011), 3, (2011), pp. 416-427
[28] Stojić, T., A Fast and Simple Method for the Visual Enhancement of Microcalcifications in Digital Mammograms Based on Mathematical Morphology, *Nucl Technol Radiat, 29* (2014), 2, pp. 108-115

Received on February 23, 2015
Accepted on March 31, 2015

**Томислав М. СТОЈИЋ**

## ВИЗУЕЛНО ИСТИЦАЊЕ МИКРОКАЛЦИФИКАЦИЈА И МАСА У ДИГИТАЛНОМ МАМОГРАМУ КОРИШЋЕЊЕМ МОДИФИКОВАНЕ МУЛТИФРАКТАЛНЕ АНАЛИЗЕ

Микрокалцификације и масе, као аномалије ткива дојке (одступања од уочене правилности околног ткива) могу се сматрати ретким догађајима у статистичком смислу на мамографском снимку. Након препознавања њихових заједничких карактеристика (светлији објекти који не припадају околном ткиву са значајним локалним контрастом само око ивице), у основни мултифрактални метод уведено је неколико модификација. Полазећи од дигиталног мамограма, предложени метод ствара одговарајуће мултифракталне слике. Додатно морфолошко постпроцесирање побољшава мултифрактални метод истицањем само региона са потенцијалним микрокалцификацијама и масама. Предложени метод је тестиран на референтним мамограмима из MiniMIAS базе. У свим тестираним случајевима, метод је успешно истакао декларисане аномалије: микрокалцификације и масе. Описан метод може се самостално користити као визуелна асистенција у клиничком испитивању мамограма, или као претпроцесирање у даљој обради мамограма у циљу сегментације, класификације и аутоматске детекције сумњивих светлих лезија у ткиву дојке.

*Кључне речи: мамографија, мултифрактална анализа, микрокалцификација, маса, обрада слике*